Conformational Characteristics of Poly(trimethylene sulfide) and Structure−Property Relationships of Representative Polysulfides and Polyethers

Yuji Sasanuma* and Akinori Watanabe

Department of Applied Chemistry and Biotechnology, Faculty of Engineering, Chiba University, 1-33 Yayoi-cho, Inage-ku, Chiba 263-8522, Japan

Received November 6, 2005; Revised Manuscript Received December 16, 2005

ABSTRACT: Conformational characteristics of poly(trimethylene sulfide) (PTMS) have been investigated by a rotational isomeric state analysis of ab initio molecular orbital calculations and ^{1}H and ^{13}C NMR experiments for a monomeric model compound, 1,3-bis(methylthio)propane, and the characteristic ratio and dipole moment ratio of the unperturbed PTMS chain. Both C−S (the first-order interaction energy, −0.30 kcal mol^{-1}) and C−C (−0.58 kcal mol^{-1}) bonds prefer the gauche conformation. For comparison, conformational analysis of the corresponding polyether, poly(trimethylene oxide), has also been carried out. The C−O (+0.97 kcal mol^{-1}) and C−C (−0.47 kcal mol^{-1}) bonds show trans and gauche preferences, respectively. These results are consistent with the conformational stabilities predicted by the natural bond orbital analysis on model compounds of poly(ethylene sulfide) (PES) and poly(ethylene oxide). Without the strong S···S repulsion, therefore, the C−C bond adjacent to the C−S bond exhibits its inherent gauche preference. Without the (C−H)···O attraction, the ethereal C−C bond is subject to the attractive gauche effect. For representative polysulfides and polyethers, relationships between conformations in the Θ and crystalline states and thermal properties have been investigated. Even in the Θ and crystalline states, the polymers mostly keep the conformational preferences found for their small model compounds; as an exception, poly(propylene sulfide) and poly(propylene oxide), having a methyl side chain, crystallize to adopt the metastable all-trans conformation. On average, the configurational entropy of the polymers amounts to 80−90% of entropy of fusion, and the configurational energy change between crystalline and molten states accounts for ca. 30% of enthalpy of fusion. Of the polymers investigated here, PES has an exceptionally high melting point; the dipole−dipole interaction in the PES crystal was evaluated to be −1.0 kcal mol^{-1} (ca. 30% of the enthalpy of fusion), thus being the source of the thermostability.

1. Introduction

In a previous study,[1] we carried out conformational analysis of poly(ethylene sulfide) (PES, $[-CH_2CH_2S-]_x$). Ab initio molecular orbital (MO) calculations and NMR experiments for its model compound, 1,2-bis(methylthio)ethane (BMTE, $CH_3SCH_2CH_2SCH_3$), showed that the C−S and C−C bonds prefer the gauche and trans states, respectively. However, natural bond orbital (NBO) analysis[2−4] on BMTE suggested that bond−antibond and lone pair−antibond interactions around the C−C and C−S bonds cause gauche stabilization in these two bonds. Therefore, it was inferred that the discrepancy about the C−C conformation stems from a strong S···S repulsion occurring in the gauche conformation because the repulsive interaction is not considered in the NBO analysis.

In this study, we have treated poly(trimethylene sulfide) (PTMS, $[-CH_2CH_2CH_2S-]_x$, Figure 1). Because the polymer has four bonds between sulfur atoms, the S···S repulsion rarely occurs, and the inherent conformational preference of the C−C bond adjacent to the C−S bond may be revealed. Semiempirical potential energy calculations on PTMS suggested that both C−S and C−C bonds have conformational energies less than 0.1 kcal mol^{-1} (i.e., the t, g$^+$, and g$^-$ states are approximately equiprobable).[5] An X-ray diffraction study on PTMS indicated that it adopts the all-gauche conformation in the crystal.[6,7]

In this study, bond conformations and conformational energies of a monomeric model compound of PTMS, 1,3-bis(methylthio)-propane (BMTP, $CH_3SCH_2CH_2CH_2SCH_3$, Figure 1), have been derived from ab initio MO calculations and NMR experiments.

* To whom correspondence should be addressed. E-mail: sasanuma@facutly.chiba-u.jp. Fax: +81 43 290 3394.

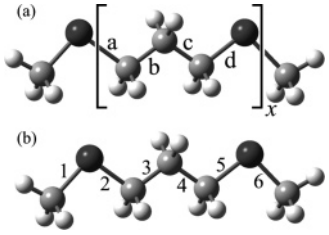

Figure 1. (a) Poly(trimethylene sulfide) (PTMS) or poly(trimethylene oxide) (PTMO) and (b) 1,3-bis(methylthio)propane (BMTP) or 1,3-dimethoxypropane (DMP). The bonds are designated as indicated.

The conformational energies were optimized so as to reproduce experimental configuration-dependent properties and bond conformations of PTMS in the Θ state. The similar procedure has been followed for the counterparts, 1,3-dimethoxypropane (DMP, $CH_3OCH_2CH_2CH_2OCH_3$) and poly(trimethylene oxide) (PTMO, $[-CH_2CH_2CH_2O-]_x$), to compare conformational characteristics of the polysulfide and polyether. In this paper, the procedures and results are reported. Furthermore, conformations, structures, and thermal properties of the polysulfides and polyethers that we have treated are compared and discussed to reveal the origin of thermostability of the polysulfides.

2. Computations and Experiments

2.1. Ab Initio MO Calculations. Ab initio MO calculations were carried out with the Gaussian03 program[8] installed on an HPC Silent-SCC T2 computer. For each conformer of BMTP and DMP, the geometrical parameters were fully optimized at the HF/6-31G-(d) level, and the thermal correction to the Gibbs free energy (at 25 °C and 1 atm) was calculated with a calibration factor of 0.9135.[9] With the optimized geometry, the self-consistent field (SCF) energy

10.1021/ma0523623 CCC: $33.50
Published on Web 01/28/2006

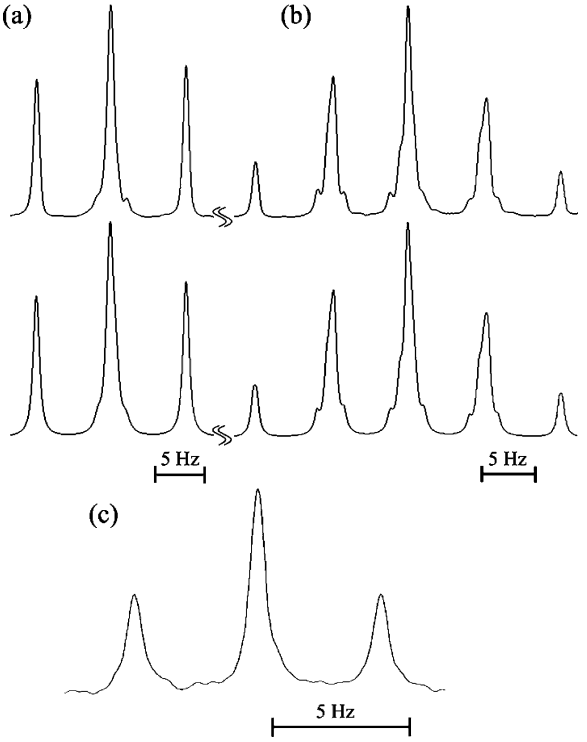

Figure 2. Observed (above) and calculated (below) ^{1}H NMR spectra of methylene protons, (a) A and A′ and (b) B and B′, of BMTP dissolved in C_6D_6 at 25 °C. (c) Observed ^{13}C NMR spectrum of methyl carbons of BMTP in $CDCl_3$ at 25 °C. For designations of the protons, see Figure 3.

was computed at the MP2/6-311+G(3df,2p) level. The SCF calculations were performed under the tight convergence. The Gibbs free energy was calculated from the SCF and thermal-correction energies, being given here as the difference from that of the all-trans conformer and denoted as ΔG_k (*k*: conformer). The computations at the B3LYP/6-311+G(3df,2p)//B3LYP/6-31G(d) level were performed similarly. Proton and carbon-13 NMR coupling constants of BMTP and a cyclic model compound, 2-*tert*-butyl-1,3- dithiane (BDT), were calculated at the HF/6-311+G(2d,p)//HF/6-31G(d) and B3LYP/6-311+G(2d,p)//B3LYP/6-31G(d) levels. For a model of PES crystal, MO calculations were performed. The details are described in section 3.7.

2.2. Sample Preparation. 1,3-Bis(methylthio)propane was purchased from Lancaster Synthesis, Inc., and used without further purification. The cyclic model compound, BDT, was prepared from pivalaldehyde and 1,3-propanedithiol with a catalyst of boron trifluoride diethyl etherate.[10]

2.3. NMR Measurements. ^{1}H (^{13}C) NMR spectra were measured at 500 MHz (126 MHz) on a JEOL JNM-LA500 spectrometer equipped with a variable temperature controller in the Chemical Analysis Center of Chiba University. During the measurement the probe temperature was maintained within ±0.1 °C fluctuations. The $\pi/2$ pulse width, data acquisition time, and recycle delay were 5.6 (5.0) μs, 3.3 (2.0) s, and 3.7 (2.0) s, respectively. Here, the values in parentheses represent the ^{13}C NMR parameters. The gated decoupling technique was employed in the ^{13}C NMR measurements. Before the Fourier transform, zero filling was performed so that the digital resolution would be close to 0.01 Hz. Cyclohexane-d_{12} (C_6D_{12}), benzene-d_6 (C_6D_6), chloroform-*d* ($CDCl_3$), methanol-d_4 (CD_3OD), and dimethyl-d_6 sulfoxide ($(CD_3)_2SO$) were used as the solvents, and the solute concentration was ca. 5 vol %.

3. Results and Discussion

3.1. ^{1}H NMR. Parts a and b of Figure 2 show ^{1}H NMR spectra observed from methylene protons of BMTP. Simulations using the gNMR program[11] yielded vicinal coupling constants, $^3J_{HH}$ ($=^3J_{AB} = {}^3J_{A'B'}$) and $^3J'_{HH}$ ($= {}^3J_{AB'} = {}^3J_{A'B}$), as listed in

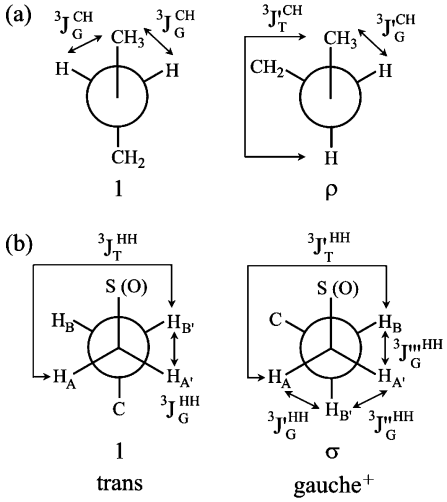

Figure 3. Conformations around (a) CH_2-S (CH_2-O) and (b) CH_2-CH_2 bonds of BMTP (DMP) and PTMS (PTMO) with definitions of vicinal coupling constants. The Greek letters represent the first-order interactions.

Table 1. Observed Vicinal ^{1}H−^{1}H and ^{13}C−^{1}H Coupling Constants of BMTP

solvent	temp (°C)	$^3J_{HH}$ (Hz)	$^3J'_{HH}$ (Hz)	$^3J_{CH}$ (Hz)
C_6D_{12}	15	7.40	6.68	4.61
	25	7.40	6.68	4.60
	35	7.40	6.68	4.59
	45	7.40	6.68	4.57
	55	7.42	6.68	4.58
C_6D_6	15	7.92	6.42	4.50
	25	7.90	6.44	4.50
	35	7.90	6.44	4.49
	45	7.88	6.40	4.49
	55	7.88	6.38	4.49
$CDCl_3$	15	7.96	6.42	4.41
	25	7.92	6.45	4.40
	35	7.86	6.48	4.41
	45	7.82	6.51	4.41
	55	7.80	6.48	4.42
CD_3OD	15	7.77	6.46	4.55
	25	7.77	6.48	4.53
	35	7.77	6.48	4.53
	45	7.78	6.48	4.52
	55	7.78	6.48	4.51
$(CD_3)_2SO$	15	8.01	6.34	4.49
	25	8.00	6.34	4.52
	35	7.98	6.33	4.50
	45	7.98	6.34	4.49
	55	7.95	6.35	4.48

Table 1. From the table, the temperature dependence of $^3J_{HH}$ and $^3J'_{HH}$ is seen to be small. The observed coupling constants can be expressed as

$$^3J_{HH} = {}^3J_G^{HH}\, p_t^{CC} + \frac{{}^3J_T^{HH} + {}^3J''_G{}^{HH}}{2}\, p_g^{CC} \qquad (1)$$

and

$$^3J'_{HH} = {}^3J_T^{HH}\, p_t^{CC} + \frac{{}^3J'_G{}^{HH} + {}^3J'''_G{}^{HH}}{2}\, p_g^{CC} \qquad (2)$$

where $^3J_T^{HH}$'s and $^3J_G^{HH}$'s are defined in Figure 3, and p_t^{CC} and p_g^{CC} are trans and gauche fractions of the C−C bond, respectively. Therefore, we have

$$p_t^{CC} + p_g^{CC} = 1 \qquad (3)$$

For $^3J^{HH}$'s of BMTP, those obtained from the $S-CH_2-CH_2-$

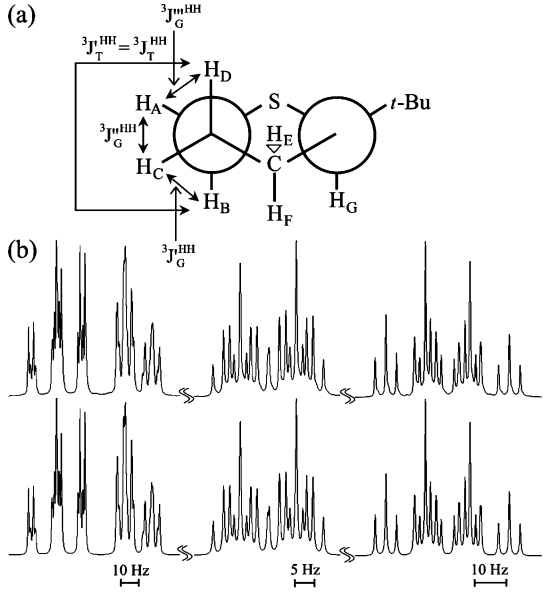

Figure 4. (a) 2-*tert*-Butyl-1,3-dithiane (BDT). (b) Observed (above) and calculated (below) ^{1}H NMR spectra of BDT dissolved in CD_3OD at 25 °C. The hydrogen atoms are designated as indicated. The NMR parameters were determined as follows (δ in ppm and J in Hz): $\delta_A - \delta_X = 1.756$, $\delta_B - \delta_X = 1.836$, $\delta_C - \delta_X = 0.972$, $\delta_D - \delta_X = 0.631$, $\delta_E - \delta_X = 1.756$, $\delta_F - \delta_X = 1.836$, $\delta_G - \delta_X = 6.311$, $^2J_{AB} = -13.96$, $^2J_{CD} = -13.86$, $^2J_{EF} = -13.96$, $^3J_{AD} = 3.10$, $^3J_{AC} = 4.19$, $^3J_{BC} = 2.51$, $^3J_{BD} = 12.57$, $^3J_{CE} = 4.19$, $^3J_{CF} = 2.51$, $^3J_{DE} = 3.10$, $^3J_{DF} = 12.57$, $^4J_{AE} = 1.44$, $^4J_{AF} = -0.41$, $^4J_{BE} = -0.41$, and $^4J_{BF} = -0.28$.

Table 2. Vicinal ^{1}H- ^{1}H Coupling Constants of BDT[a]

solvent or method	$^3J^{HH}_T$	$^3J^{HH}_G$	$^3J'^{HH}_G$	$^3J''^{HH}_G$	$^3J^{HH}_G$
	NMR experiment[b]				
C_6D_{12}	12.50	2.45	4.28	3.10	3.28
C_6D_6	12.74	2.61	4.16	2.91	3.23
$CDCl_3$	12.19	2.40	4.37	3.54	3.44
CD_3OD	12.57	2.51	4.19	3.10	3.27
$(CD_3)_2SO$	12.59	2.49	4.25	3.03	3.26
	MO calculation[c]				
B3LYP/6-311+G(2d,p)	11.15	2.42	4.21	3.04	3.22
HF/6-311+G(2d,p)	13.72	4.33	6.08	4.88	5.10

[a] In Hz. For definitions of the coupling constants, see Figure 4a. $^3J^{HH}_T = {}^3J'^{HH}_T$ and $^3J^{HH}_G = (^3J^{HH}_G + {}^3J''^{HH}_G + {}^3J''^{HH}_G)/3$. [b] At 25 °C. [c] Calculated with the Gaussian03 program.[8]

CH_2-S bond sequence of BDT (Figure 4a) have been substituted; the 2-*tert*-butyl group prevents the dithian ring from flip-flopping. Figure 4b shows an example of observed and calculated ^{1}H NMR spectra of BDT. In Table 2, the vicinal coupling constants derived from the gNMR simulations are listed and compared with the MO calculations. The p^{CC}_t and p^{CC}_g values were derived from eqs 1 and 2, and divided by their sum to satisfy eq 3, as in previous studies.[1,12,13] Because of the slight temperature dependence of p^{CC}_t and p^{CC}_g, only the trans fractions at 25 °C are shown in the column "case I" of Table 3.

As seen from Table 2, the MO calculations at the B3LYP/6-311+G(2d,p) level successfully reproduced the experimental $^3J^{HH}$ values. Density functional calculations at a higher level of B3LYP/6-311+G(3df,2p) for BMTP itself yielded the $^3J^{HH}_T$ and $^3J^{HH}_G$ values of eqs 1 and 2 as $^3J^{HH}_T = 11.93$, $^3J'^{HH}_T = 11.84$, $^3J^{HH}_G = 3.85$, $^3J'^{HH}_G = 2.58$, $^3J''^{HH}_G = 4.22$, and $^3J'''^{HH}_G = 2.94$ Hz. From these data and the experimental $^3J_{HH}$'s and $^3J'_{HH}$'s, the trans fractions were obtained as shown in column "case II" of Table 3. The results agree well with those of case I. The p^{CC}_t values indicate the flexibility of the C−C bond: for example, $p^{CC}_t = 0.34$ leads to $p^{CC}_{g+} = p^{CC}_{g-} = 0.33$. In the table, bond conformations of BMTP, calculated from the ab initio MO calculations, are compared with the NMR observations.

3.2. ^{13}C NMR. Figure 2c shows an observed ^{13}C NMR spectrum of the methyl carbon of BMTP. The triplet is due to the vicinal coupling ($^3J_{CH}$) between the methyl carbon and methylene protons, A and A′. The $^3J_{CH}$ values for the five solutions are listed in Table 1. The observed $^3J_{CH}$ value is expressed as

$$^3J_{CH} = {}^3J^{CH}_G p^{CS}_t + \frac{{}^3J'^{CH}_T + {}^3J'^{CH}_G}{2} p^{CS}_g \qquad (4)$$

where $^3J^{CH}$'s are defined in Figure 3, and p^{CS}_t and p^{CS}_g are trans and gauche fractions of the C−S bond, respectively. Accordingly, we have

$$p^{CS}_t + p^{CS}_g = 1 \qquad (5)$$

On the assumption that $^3J^{CH}_G = {}^3J'^{CH}_G$, the p^{CS}_t values were calculated with the $^3J^{CH}_T$ ($^3J'^{CH}_T$) and $^3J^{CH}_G$ values[1] determined from 2-methyl-1,3,5-trithiane[14] (for the numerical data, see the footnote of Table 3). The p^{CS}_t values of the solutions at 25 °C are listed in the column "case I" of Table 3.

The vicinal ^{13}C−^{1}H coupling constants of BMTP were evaluated from density functional calculations at the B3LYP/6-311+G(3df,2p) level: $^3J^{CH}_G = 1.78$ Hz, $^3J'^{CH}_T = 7.40$ Hz, and $^3J'^{CH}_G = 3.41$ Hz. The $^3J'^{CH}_T$ and averaged $^3J^{CH}_G$ [(1.78 + 3.41)/2 = 2.60] values are very close to those observed from 2-methyl-1,3,5-trithiane. Adoption of the calculated $^3J^{CH}$ values leads to p^{CS}_t's as shown in the column "case II" of Table 3. The trans fractions are somewhat larger than those of case I but closer to the MO calculations; therefore, the p^{CS}_t data of case II have been adopted here. It has been proven that the density functional calculations yield the reliable ^{1}H−^{1}H and ^{13}C−^{1}H coupling constants. The p^{CS}_t's of BMTP are close to those (0.12−0.26) of BMTE.[1] Table 3 also shows trans fractions of C−C and C−O bonds of DMP; the data were taken from ref 15. The C−C and C−O bonds prefer gauche and trans conformations, respectively.

3.3. Statistical Weight Matrixes and Conformational Energies of BMTP and DMP. Statistical weight matrices, U_i (i, bond number), of BMTP and DMP were formulated according to the 9 × 9 matrix scheme:

$$U_2 = \begin{bmatrix} 1 & \rho & \rho \\ 0 & 0 & 0 \\ 0 & 0 & 0 \end{bmatrix} \qquad (6)$$

$$U_3 = \begin{bmatrix} 1 & \sigma & \sigma & 0 & 0 & 0 & 0 & 0 & 0 \\ 0 & 0 & 0 & 1 & \sigma & \sigma\omega & 0 & 0 & 0 \\ 0 & 0 & 0 & 0 & 0 & 0 & 1 & \sigma\omega & \sigma \end{bmatrix} \qquad (7)$$

$$U_4 = \begin{bmatrix} 1 & \sigma & \sigma & 0 & 0 & 0 & 0 & 0 & 0 \\ 0 & 0 & 0 & 1 & \sigma & \sigma\omega' & 0 & 0 & 0 \\ 0 & 0 & 0 & 0 & 0 & 0 & 1 & \sigma\omega' & \sigma \\ 1 & \sigma & \sigma & 0 & 0 & 0 & 0 & 0 & 0 \\ 0 & 0 & 0 & 1 & \sigma & \sigma\omega' & 0 & 0 & 0 \\ 0 & 0 & 0 & 0 & 0 & 0 & 1 & 0 & \sigma \\ 1 & \sigma & \sigma & 0 & 0 & 0 & 0 & 0 & 0 \\ 0 & 0 & 0 & 1 & \sigma & 0 & 0 & 0 & 0 \\ 0 & 0 & 0 & 0 & 0 & 0 & 1 & \sigma\omega' & \sigma \end{bmatrix} \qquad (8)$$

and

$$U_5 = \begin{bmatrix} 1 & \rho & \rho & 0 & 0 & 0 & 0 & 0 & 0 \\ 0 & 0 & 0 & 1 & \rho & \rho\omega & 0 & 0 & 0 \\ 0 & 0 & 0 & 0 & 0 & 0 & 1 & \rho\omega & \rho \\ 1 & \rho & \rho & 0 & 0 & 0 & 0 & 0 & 0 \\ 0 & 0 & 0 & 1 & \rho & \rho\omega & 0 & 0 & 0 \\ 0 & 0 & 0 & 0 & 0 & 0 & 1 & 0 & \rho \\ 1 & \rho & \rho & 0 & 0 & 0 & 0 & 0 & 0 \\ 0 & 0 & 0 & 1 & \rho & 0 & 0 & 0 & 0 \\ 0 & 0 & 0 & 0 & 0 & 0 & 1 & \rho\omega & \rho \end{bmatrix} \quad (9)$$

The rows and columns of the above matrices correspond to the rotational states for the preceding and current bonds, respectively. For the intramolecular interactions defined here, see Figures 3 and 5. The statistical weight is related to the corresponding conformational energy through the Boltzmann factor; for example, $\rho = \exp(-E_\rho/RT)$. In the rotational isomeric state (RIS) scheme,[16,17] the ΔG_k values of BMTP and DMP (Table 4) may be approximated as a function of E_ξ's ($\xi = \rho$, σ, and ω's). The E_ξ values were determined by minimizing the following function:

$$S(\boldsymbol{E}) = \frac{1}{K}\sum_{k}^{K}\left[\sum_{\xi} L(\xi)E_\xi - \Delta G_k\right]^2 M_k \quad (10)$$

The function $L(\xi)$ gives the number of conformational energy E_ξ included in the conformer, and M_k is the multiplicity of the conformation. The temperature T was set to 298.15 K. The conformational energies thus determined are listed in the column "ΔG_k" of Table 5.

From Table 4, it can be seen that conformers of BMTP with the same statistical weight have different ΔG_k values. The weights and the ΔG_k and μ_k values of the relevant conformers are as follows: weight $\sigma\rho$, conformers 4 (-0.59 kcal mol^{-1}, 0.33 D), 6 (-0.40 kcal mol^{-1}, 2.00 D), and 7 (-0.18 kcal mol^{-1}, 3.13 D); ρ^2, conformers 14 (-0.53 kcal mol^{-1}, 0.21 D) and 15 (-0.37 kcal mol^{-1}, 2.34 D); $\sigma\rho^2$, conformers 16 (-0.59 kcal mol^{-1}, 2.01 D) and 19 (-0.61 kcal mol^{-1}, 2.23 D); $\sigma\rho^2\omega$, conformers 17 (0.56 kcal mol^{-1}, 0.76 D) and 18 (0.77 kcal mol^{-1}, 2.57 D). A definite correlation can be found between ΔG_k and μ_k; the ΔG_k value increases with μ_k. This tendency can also be seen for DMP, although it is weaker than that of BMTP. On the assumption that the ΔG_k difference may come from the dipole potential ($E_{\mathrm{dip},k}$) similar to the Born energy,[18] the ΔG_k values were attempted to be analyzed.

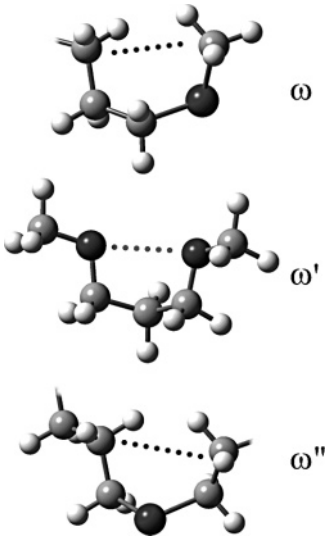

Figure 5. Second-order interactions of BMTP (DMP) and PTMS (PTMO).

The dipole potential is given by[19]

$$E_{\mathrm{dip},k} = \frac{{\mu_k}^2}{4\pi\epsilon_0\epsilon_r {l_k}^3} \quad (11)$$

where ϵ_0 is the electric constant, ϵ_r is the dielectric constant, and l_k is the dipole distance. The dipole moment of a conformer stems from its overall unbalanced charge distribution. However, the treatment employed here is coarser; the dipole moment is assumed to arise from a pair of imaginary point charges, $+q_k$ and $-q_k$, separated by l_k: $\mu_k = q_k l_k$. The conformer free energy is given as the sum of the dipole potential and the net conformer energy ($E_{\mathrm{conf},k}$):

$$G_k = E_{\mathrm{dip},k} + E_{\mathrm{conf},k} \quad (12)$$

Table 3. Bond Conformations of BMTP and DMP

				p_t^{CC}		p_t^{CX}	
method	solvent	permittivity	temp, °C	case I[a]	case II[b]	case I[c]	case II[d]
				BMTP (X = S)			
MO[e]	(gas)	1.0	25	0.44		0.34	
NMR	C_6D_{12}	2.0	25	0.34	0.35	0.12	0.22
	C_6D_6	2.3	25	0.29	0.30	0.17	0.25
	$CDCl_3$	4.8	25	0.29	0.30	0.20	0.28
	CD_3OD	32.7	25	0.30	0.31	0.16	0.24
	$(CD_3)_2SO$	46.7	25	0.28	0.29	0.14	0.24
				DMP (X = O)			
MO[e]	(gas)	1.0	25	0.22		0.89	
			40	0.23		0.87	
			160	0.30		0.78	
NMR[f]	(gas)	1.0	160	0.26		0.73	
	C_6D_{12}	2.0	40	0.25		0.81	
	$(CD_3)_2CO$	20.7	40	0.31		0.78	
	CD_3OD	32.7	40	0.29		0.78	

[a] Evaluated from the $^3J_{HH}$ and $^3J'_{HH}$ values (Table 1) using the experimental $^3J_T^{HH}$, $^3J_T'^{HH}$, $^3J_G^{HH}$, $^3J_G'^{HH}$, $^3J_G''^{HH}$, and $^3J_G'''^{HH}$ values of BDT (Table 2). [b] Using the ^3J values obtained from MO calculations for BMTP itself at the B3LYP/6-311+G(3df,2p)//B3LYP/6-31G(d) level: $^3J_T^{HH} = 11.93$, $^3J_T'^{HH} = 11.84$, $^3J_G^{HH} = 3.85$, $^3J_G'^{HH} = 2.58$, $^3J_G''^{HH} = 4.22$, and $^3J_G'''^{HH} = 2.94$ Hz. [c] Evaluated from the $^3J_{CH}$ values (Table 1) using the experimental $^3J_T^{CH}$ and $^3J_G^{CH}$ values of 2-methyl-1,3,5-trithiane:[14] C_6D_{12} and C_6D_6, $^3J_T^{CH} = 7.13$ and $^3J_G^{CH} = 2.62$ Hz; $CDCl_3$, $^3J_T^{CH} = 7.12$ and $^3J_G^{CH} = 2.58$ Hz; CD_3OD, $^3J_T^{CH} = 7.27$ and $^3J_G^{CH} = 2.54$ Hz; $(CD_3)_2SO$, $^3J_T^{CH} = 6.92$ and $^3J_G^{CH} = 2.71$ Hz. [d] Using the ^3J values obtained from MO calculations for BMTP itself at the B3LYP/6-311+G(3df,2p)//B3LYP/6-31G(d) level: $^3J_T^{CH} = 7.40$, $^3J_G^{CH} = 1.78$, and $^3J_G'^{CH} = 3.41$ Hz. [e] Calculated from the conformer free energies (Table 4). [f] Reference 15.

Table 4. Conformer Free Energies of BMTP and DMP, Evaluated from ab Initio MO Calculations

				ΔG_k[a], kcal mol^{-1}	
k	conformation	M_k	statistical weight[b]	BMTP	DMP
1	t t t t	1	1	0.00	0.00
2	t t t g$^+$	4	ρ	−0.31	1.03
3	t t g$^+$ t	4	σ	−0.15	−0.88
4	t t g$^+$ g$^+$	4	$\sigma\rho$	−0.59	0.22
5	t t g$^+$ g$^-$	4	$\sigma\rho\omega$ (0)	0.84	
6	t g$^+$ t g$^+$	4	$\sigma\rho$	−0.40	0.25
7	t g$^+$ t g$^-$	4	$\sigma\rho$	−0.18	0.48
8	t g$^+$ g$^+$ t	2	σ^2	−0.39	−1.67
9	t g$^+$ g$^+$ g$^+$	4	$\sigma^2\rho$	−0.67	−0.20
10	t g$^+$ g$^+$ g$^-$	4	$\sigma^2\rho\omega$ (0)	0.03	
11	t g$^+$ g$^-$ t	2	0 ($\sigma^2\omega'$)		1.44
12	t g$^+$ g$^-$ g$^+$	4	0		
13	t g$^+$ g$^-$ g$^-$	4	0 ($\sigma^2\rho\omega'$)		1.70
14	g$^+$ t t g$^+$	2	ρ^2	−0.53	2.10
15	g$^+$ t t g$^-$	2	ρ^2	−0.37	2.23
16	g$^+$ t g$^+$ g$^+$	4	$\sigma\rho^2$	−0.59	1.54
17	g$^+$ t g$^+$ g$^-$	4	$\sigma\rho^2\omega$ (0)	0.56	
18	g$^+$ t g$^-$ g$^+$	4	$\sigma\rho^2\omega$ (0)	0.77	
19	g$^+$ t g$^-$ g$^-$	4	$\sigma\rho^2$	−0.61	1.52
20	g$^+$ g$^+$ g$^+$ g$^+$	2	$\sigma^2\rho^2$	−0.87	1.49
21	g$^+$ g$^+$ g$^+$ g$^-$	4	0		
22	g$^+$ g$^+$ g$^-$ g$^+$	4	0		
23	g$^+$ g$^+$ g$^-$ g$^-$	2	0 ($\sigma^2\rho^2\omega'$)		3.70
24	g$^+$ g$^-$ g$^+$ g$^-$	2	0		
25	g$^+$ g$^-$ g$^-$ g$^+$	2	0		

[a] At the MP2/6-311+G(3df,2p)//HF/6-31G(d) level. Relative to the G_k value of the all-trans conformation. The blank indicates that the geometrical optimization did not detect the potential minimum; thus, the conformer is considered to be absent, and the null statistical weight is assigned thereto. [b] The symbols in the parentheses represent statistical weights for DMP. For interactions corresponding to the statistical weights, see Figures 3 and 5.

Table 5. Conformational Energies (kcal mol^{-1}) of BMTP (PTMS) and DMP (PTMO)

	BMTP (PTMS)			DMP (PTMO)		
	MO[a]			MO[a]		
	ΔG_k[b]	$E_{\mathrm{conf},k}$[c]	exptl[d]	ΔG_k[b]	$E_{\mathrm{conf},k}$[c]	exptl[d]
	First-Order Interaction					
E_ρ	−0.17	−0.11	−0.30	1.13	1.15	0.97
E_σ	−0.27	−0.19	−0.58	−0.71	−0.65	−0.47
	Second-Order Interaction					
E_ω	1.13	1.16	0.43	∞	∞	∞
$E_{\omega'}$	∞	∞	∞	2.41	2.38	0.39
$E_{\omega''}$	0.53		0.48	∞		∞

[a] At the MP2/6-311+G(3df,2p)//HF/6-31G(d) level. [b] From the ΔG_k values (Table 4). [c] From the $E_{\mathrm{conf},k}$ values (Table 6). [d] From the RIS simulation for experimental $\langle r^2\rangle_0/nl^2$, $\mathrm{d}(\ln\langle r^2\rangle_0)/\mathrm{d}T$, $\langle\mu^2\rangle/nm^2$, $\mathrm{d}(\ln\langle\mu^2\rangle)/\mathrm{d}T$, p_t^{CX}, (X = S or O) and p_t^{CC} values.

Then, ΔG_k is given by

$$\Delta G_k = (E_{\mathrm{dip},k} - E_{\mathrm{dip},1}) + (E_{\mathrm{conf},k} - E_{\mathrm{conf},1}) \qquad (13)$$

where $k = 1$ represents the all-trans conformer, and hence $E_{\mathrm{conf},1} = 0$ and $\Delta G_1 = 0$. The dipole distance is approximated as

$$l_k = \alpha\, a_{0,k} \qquad (14)$$

where $a_{0,k}$ is the conformer radius of Onsager's model (Table 6),[20,21] and α is the proportionality factor. In Onsager's model, the conformer is assumed to be spherical. The α value was adjusted so as to minimize

$$\sum_{k'}\sum_{k}(E_{\mathrm{conf},k} - E_{\mathrm{conf},k'}) \quad (k' \neq k)$$

where k and k' represent the conformers having the same statistical weight. The $E_{\mathrm{dip},k}$ term was calculated from the optimum α value, and, consequently, the $E_{\mathrm{conf},k}$ term was separated from ΔG_k. The results are shown in Table 6. The optimum α values are 1.64 for BMTP and 1.71 for DMP, indicating that l_k is larger than the conformer radius ($\alpha = 1$) and smaller than the diameter ($\alpha = 2$). These results are reasonable because the dipole moment is encased within the conformer. The net conformational energies were determined by substituting $E_{\mathrm{conf},k}$'s for ΔG_k's in eq 10, being shown in column "$E_{\mathrm{conf},k}$" of Table 5. The E_ρ and E_σ values of BMTP are −0.11 and −0.19 kcal mol^{-1}, respectively. These small conformational energies are fairly consistent with the semiempirical potential energy calculations in the previous study.[5] The present analysis is indicative of the significance of the dipole-moment effect on the conformation of thioethers in vacuo. As eq 11 indicates, however, the dipole potential is reduced by a factor of ϵ_r^{-1}, thus being negligible in polar solvents or considered as a part of solvation energy.

3.4. Statistical Weight Matrixes, Characteristic Ratios, and Dipole Moment Ratios of PTMS and PTMO. Statistical weight matrices for bonds a and b (see Figure 1) of PTMS and PTMO may be expressed as

$$U_a = \begin{bmatrix} 1 & \rho & \rho & 0 & 0 & 0 & 0 & 0 & 0 \\ 0 & 0 & 0 & 1 & \rho & \rho\omega'' & 0 & 0 & 0 \\ 0 & 0 & 0 & 0 & 0 & 0 & 1 & \rho\omega'' & \rho \\ 1 & \rho & \rho & 0 & 0 & 0 & 0 & 0 & 0 \\ 0 & 0 & 0 & 1 & \rho & \rho\omega'' & 0 & 0 & 0 \\ 0 & 0 & 0 & 0 & 0 & 0 & 1 & 0 & \rho \\ 1 & \rho & \rho & 0 & 0 & 0 & 0 & 0 & 0 \\ 0 & 0 & 0 & 1 & \rho & 0 & 0 & 0 & 0 \\ 0 & 0 & 0 & 0 & 0 & 0 & 1 & \rho\omega'' & \rho \end{bmatrix} \qquad (15)$$

$$U_b = \begin{bmatrix} 1 & \sigma & \sigma & 0 & 0 & 0 & 0 & 0 & 0 \\ 0 & 0 & 0 & 1 & \sigma & \sigma\omega & 0 & 0 & 0 \\ 0 & 0 & 0 & 0 & 0 & 0 & 1 & \sigma\omega & \sigma \\ 1 & \sigma & \sigma & 0 & 0 & 0 & 0 & 0 & 0 \\ 0 & 0 & 0 & 1 & \sigma & \sigma\omega & 0 & 0 & 0 \\ 0 & 0 & 0 & 0 & 0 & 0 & 1 & 0 & \sigma \\ 1 & \sigma & \sigma & 0 & 0 & 0 & 0 & 0 & 0 \\ 0 & 0 & 0 & 1 & \sigma & 0 & 0 & 0 & 0 \\ 0 & 0 & 0 & 0 & 0 & 0 & 1 & \sigma\omega & \sigma \end{bmatrix} \qquad (16)$$

For bonds c and d, we have $U_c = U_4$ and $U_d = U_5$. The ω'' interaction does not appear in the monomers; therefore, the $E_{\omega''}$ values were evaluated from the MO calculations for dimers $CH_3X(CH_2)_3X(CH_2)_3XCH_3$ (X = S or O). For X = S, $E_{\omega''}$ was obtained as 0.53 kcal mol^{-1}. For X = O, however, no potential minimum was found; thus, $E_{\omega''}$ has been considered to be ∞. This difference stems form that in the C−X bond length: $l_{CS} = 1.84$ and $l_{CO} = 1.42$ Å.

Geometrical parameters of BMTP and DMP, optimized by the MO calculations at the B3LYP/6-31G(d) level, were used for PTMS and PTMO, respectively (Table 7). Bond dipole moments, m_{C-S} and m_{C-O}, were determined from MO calculations as described previously.[22] Then, μ_k's at the B3LYP/6-311+G(3df,2p)//B3LYP/6-31G(d) level and ΔG_k's at the MP2/6-311+G(3df,2p)//HF/6-31G(d) level were employed because this combination has yielded reliable results for polysulfides and polyethers. The optimum values of $m_{C-S} = 1.22$ D (for PTMS) and $m_{C-O} = 1.17$ D (for PTMO) are consistent with the previous studies: poly(methylene sulfide) (PMS),[14] 1.23 D; PES,[1] 1.22 D; poly(propylene sulfide) (PPS),[23] 1.21 D; poly-

Table 6. Dipole Moments, Conformer Radii, Dipole Energies, and Net Conformational Energies of BMTP and DMP

		BMTP				DMP			
k	conformation	μ_k[a] (D)	$a_{0,k}$[a,b] (Å)	$E_{\mathrm{dip},k}$ (kcal mol^{-1})	$E_{\mathrm{conf},k}$ (kcal mol^{-1})	μ_k[a] (D)	$a_{0,k}$[a,b] (Å)	$E_{\mathrm{dip},k}$ (kcal mol^{-1})	$E_{\mathrm{conf},k}$ (kcal mol^{-1})
1	t t t t	3.06	4.54	0.32	0.00	2.31	4.15	0.21	0.00
2	t t t g$^+$	2.16	4.34	0.19	−0.17	1.76	4.30	0.11	1.14
3	t t g$^+$t	2.08	4.51	0.15	0.02	1.63	4.21	0.10	−0.77
4	t t g$^+$g$^+$	0.33	4.39	0.00	−0.27	0.23	4.08	0.00	0.44
5	t t g$^+$ g$^-$	2.26	4.47	0.19	0.97				
6	t g$^+$ t g$^+$	2.00	4.42	0.15	−0.22	1.69	4.29	0.10	0.36
7	t g$^+$ t g$^-$	3.13	4.34	0.39	−0.25	2.46	4.11	0.25	0.45
8	t g$^+$ g$^+$ t	0.09	4.32	0.00	−0.07	0.20	4.18	0.00	−1.46
9	t g$^+$ g$^+$ g$^+$	2.00	4.50	0.14	−0.49	1.49	4.11	0.09	−0.08
10	t g$^+$ g$^+$ g$^-$	1.46	4.39	0.08	0.28				
11	t g$^+$ g$^-$ t					1.71	4.26	0.11	1.55
12	t g$^+$ g$^-$ g$^+$								
13	t g$^+$ g$^-$ g$^-$					1.35	4.17	0.07	1.84
14	g$^+$ t t g$^+$	0.21	4.54	0.02	−0.21	0.07	4.10	0.00	2.32
15	g$^+$ t t g$^-$	2.34	4.50	0.20	−0.24	2.11	4.24	0.17	2.27
16	g$^+$ t g$^+$ g$^+$	2.01	4.48	0.15	−0.41	1.88	4.04	0.15	1.60
17	g$^+$ t g$^+$ g$^-$	0.76	4.33	0.02	0.86				
18	g$^+$ t g$^-$ g$^+$	2.57	4.56	0.23	0.87				
19	g$^+$ t g$^-$ g$^-$	2.23	4.45	0.18	−0.47	1.81	4.19	0.13	1.61
20	g$^+$ g$^+$ g$^+$ g$^+$	3.12	4.47	0.35	−0.90	2.47	4.16	0.24	1.46
21	g$^+$ g$^+$ g$^+$ g$^-$								
22	g$^+$ g$^+$ g$^-$ g$^+$								
23	g$^+$ g$^+$ g$^-$ g$^-$					2.37	4.21	0.22	3.69
24	g$^+$ g$^-$ g$^+$ g$^-$								
25	g$^+$ g$^-$ g$^-$ g$^+$								

[a] At the B3LYP/6-311+G(3df,2p)//B3LYP/6-31G(d) level. [b] The radius recommended for Onsager's model.

Table 7. Geometrical Parameters Used in the RIS Simulations[a]

	PTMS (X = S)	PTMO (X = O)
	bond length, Å	
l_{CX}	1.84	1.42
l_{CC}	1.53	1.52
	bond angle, °	
∠CXC	99.5	112.8
∠XCC	110.3	108.3
∠CCC	111.4	112.7
	dihedral angle[b], °	
$\phi_{\mathrm{g}\pm}^{\mathrm{CX}}$	±108.3	±103.7
$\phi_{\mathrm{g}\pm}^{\mathrm{CC}}$	±115.1	±118.6
	bond dipole moment[c], D	
$m_{\mathrm{C-X}}$	1.22	1.17

[a] Determined by the geometrical optimizations for BMTP and DMP at the B3LYP/6-31G(d) level. [b] $\phi_{\mathrm{t}}^{\mathrm{CX}} = \phi_{\mathrm{t}}^{\mathrm{CC}} = 0.0°$. [c] $m_{\mathrm{C-C}} = 0.00$ D.

(propylene oxide) (PPO) and poly(tetramethylene oxide),[24] 1.17−1.19 D; poly(ethylene oxide) (PEO),[1] 1.18 D. The bond dipole moment of the C−C bond has been assumed to be null.

From the above-mentioned statistical weight matrices, the geometrical parameters, and the conformational energies in the column of "ΔG_k" of Table 5, the characteristic ratio and dipole moment ratio were calculated as follows: $\langle r^2\rangle_0/nl^2$, 4.8 (PTMS) and 4.8 (PTMO); $\langle \mu^2\rangle/nl^2$, 0.68 (PTMS) and 0.23 (PTMO). The results differ somewhat from the experiments (Table 8). Accordingly, the energy parameters were adjusted so as to reproduce the observed molecular parameters, viz., the characteristic ratio, the dipole moment ratio, their temperature coefficients, and the bond conformations. To minimize the influence of solvent polarity, the data observed with the identical or similar (nonpolar) solvents were adopted in the simulations. The initial energies were set as in column "ΔG_k" of Table 5. For PTMS (PTMO), the four (three) energies were optimized for the 13 (12) experimental data and, as a consequence, determined uniquely as shown in column "exptl" of Table 5.

The results of the simulations (Table 8) are seen to agree with the experiments except for $\mathrm{d}(\ln\langle\mu^2\rangle)/\mathrm{d}T$ of PTMS. In a previous study,[30,31] the dipole moment ratios of PTMS were calculated from the semiempirical potential energy calculations, and a negative $\mathrm{d}(\ln\langle\mu^2\rangle)/\mathrm{d}T$ value was also obtained even though a 5-state model was employed. Listed in Table 9 are first derivatives ($|X|^{-1}(\partial X/\partial E_\xi)$) of the configuration-dependent properties and bond conformations (X's) of PTMS and PTMO with respect to the conformational energies (E_ξ's). The magnitude represents the sensitivity of the molecular parameter to the energy variation. The temperature coefficient, $\mathrm{d}(\ln\langle\mu^2\rangle)/\mathrm{d}T$, largely depends on E_ρ, E_ω, and E_ω''. Although we attempted to reproduce the experimental $\mathrm{d}(\ln\langle\mu^2\rangle)/\mathrm{d}T$ value selectively, we could obtain only unreasonable energy sets. Then, the other molecular parameters calculated concomitantly were far from satisfactory. It should be noted that the present simulations fairly reproduced the temperature dependence of $p_{\mathrm{t}}^{\mathrm{CX}}$ and $p_{\mathrm{t}}^{\mathrm{CC}}$. Therefore, the experimental $\mathrm{d}(\ln\langle\mu^2\rangle)/\mathrm{d}T$ value may not result only from the configurational change of the polymeric chain. For PTMS, the two first-order interaction energies suggest that the gauche states are more stable in the solutions than in vacuo. The second-order interaction energy E_ω was considerably changed from 1.13 to 0.43 kcal mol^{-1}. As seen from Table 9, E_ω has large efffects on all the molecular parameters and hence has little tolerance. The optimized E_ω value of 0.43 kcal mol^{-1} is almost equal to that (0.40−0.53 kcal mol^{-1}) of PES.[1]

For PTMO, E_ρ and E_σ were, respectively, obtained as +0.97 and −0.47 kcal mol^{-1}, being consistent with previous analyses.[15,33,34] In PTMO, no intramolecular hydrogen bonds are formed; thus, it is obvious that the negative E_σ stems from the attractive gauche effect[35,36] as predicted by the NBO analysis for 1,2-dimethoxyethane.[1] In a previous study,[34] the E_ω' value was found to change with permittivity (ϵ_{r}) by semiempirical potential energy calculations: the E_ω' value was reduced from 1.97 to 0.82 kcal mol^{-1} with an increase in ϵ_{r} from 1.0 to 3.0. Adoption of $E_\omega = 0.40$ kcal mol^{-1} gave good agreement between theory and experiment.[15] These results are consistent

Table 8. Observed and Calculated Values of Configuration-Dependent Properties and Bond Conformations of PTMS (BMTP) and PTMO (DMP)

	PTMS (BMTP)				PTMO (DMP)			
	solvent	temp (°C)	obsd[a]	calcd[b]	solvent	temp (°C)	obsd[a]	calcd[b]
				Polymer				
$\langle r^2\rangle_0/nl^2$	$CHCl_3$	25	3.9 ± 0.3[c]	3.6	C_6H_{12}	27	3.9 ± 0.3[d]	3.7
$d(\ln\langle r^2\rangle_0)/dT \times 10^3$, K^{-1}		25	-	−0.5	amorphous	60	0.08[e]	0.6
$\langle\mu^2\rangle/nm^2$	C_6H_6	30	0.60[f]	0.63	CCl_4	20	0.35[g]	0.32
$d(\ln\langle\mu^2\rangle)/dT \times 10^3$, K^{-1}	C_6H_6	40	1.3[f]	−0.3	CCl_4	35	1.8[g]	1.9
p_t^{CX}		25	-	0.34		25	-	0.82
p_t^{CC}		25	-	0.29		25	-	0.24
				Monomeric Model				
p_t^{CX}	$CDCl_3$[h]	15	0.28	0.27	C_6D_{12}[i]	25	0.82	0.81
		25	0.28	0.27		40	0.81	0.80
		35	0.28	0.27		60	0.79	0.78
		45	0.28	0.28		80	0.77	0.76
		55	0.27	0.28				
p_t^{CC}	$CDCl_3$[h]	15	0.28	0.28	C_6D_{12}[i]	25	0.24	0.25
		25	0.29	0.28		40	0.25	0.25
		35	0.29	0.29		60	0.26	0.26
		45	0.30	0.29		80	0.26	0.27
		55	0.30	0.29				

[a] The blanks stand for unavailable data. The original $\langle r^2\rangle_0/nl^2$ and $\langle\mu^2\rangle/nm^2$ values were modified with the bond lengths and bond dipole moments shown in Table 7. The allowance of $\langle r^2\rangle_0/nl^2$ is due to that ($(2.3-2.8) \times 10^{23}$ mol^{-1}) of the viscosity constant, Φ.[25,26] [b] Results of the simulations for the observed data. The optimized energy parameters are listed in columns of "exptl" of Table 5. [c] Estimated from intrinsic viscosities of PTMS in a good solvent, $CHCl_3$.[27] [d] Determined from the Θ solution.[28] A value of 4.0 was also estimated from the benzene (good solvent) solution at 30 °C.[29] [e] Obtained from elasticities of the amorphous network.[29] [f] References 30 and 31. [g] References 31 and 32. [h] This study. [i] Reference 15.

Table 9. First Derivatives $|X|^{-1}(\partial X/\partial E_\xi)$ of Configuration-Dependent Properties and Bond Conformations of PTMS and PTMO with Respect to Conformational Energies (E_ξ's)[a]

	X					
E_ξ	$\langle r^2\rangle_0/nl^2$[b]	$d(\ln\langle r^2\rangle_0)/dT$[c]	$\langle\mu^2\rangle/nm^2$[b]	$(d\ln\langle\mu^2\rangle)/dT$[c]	p_t^{CX}[b,d]	p_t^{CC}[b,d]
			PTMS			
E_ρ	210	220	−260	5800	1200	−61
E_σ	87	500	69	260	−63	1100
E_ω	550	−3700	−260	−2800	290	250
$E_{\omega''}$	67	−310	−90	1300	0	0
			PTMO			
E_ρ	−80	47	−280	340	260	−140
E_σ	700	−2300	750	−1500	−44	1200
$E_{\omega'}$	550	−2200	−25	370	−12	320

[a] At each temperature (Table 8) and E_ξ value ("exptl" of Table 5). The other energies were set as in column "exptl" of Table 5. [b] In 10^{-3} $kcal^{-1}$ mol. [c] In 10^{-3} K^{-1} $kcal^{-1}$ mol. [d] At 25 °C.

with the present study. As inferred previously,[1] the discrepancies in the C−C conformations of PES and PEO between the NBO analysis and experiments are, respectively, due to the strong S···S repulsion and the intramolecular (C−H)···O attractions because these interactions are not considered in the NBO analysis. Accordingly, it can be concluded that the C−C bonds adjacent to the C−S and C−O bonds have the inherent gauche preferences to a greater or lesser extent.

For a model compound of poly(pentamethylene sulfide), $CH_3S(CH_2)_5SCH_3$, ab initio MO calculations at the MP2/6-311+G(3df,2p)//HF/6-31G(d) level were carried out, and the ΔG_k values of the gttttt, tgtttt, and ttgttt conformers were obtained as −0.18 (−0.31), 0.03 (−0.15), and 0.46 kcal mol^{-1}, respectively. The values in the parentheses are the corresponding ΔG_k's of BMTP. The magnitudes of the gauche preferences seem to depend on the number of methylene units between sulfur atoms.

3.5. Crystal Structures of PTMS and PTMO. The PTMS chain crystallizes to adopt the all-gauche conformation (gggg) of the same sign and form a monoclinic (P_c-C_s^2) unit cell of $a = 5.16$, b (fiber axis) $= 4.06$, $c = 10.33$ Å, and $\beta = 120.5°$.[6,7] The unit cell includes two monomeric units and two chains. In the crystal, therefore, PTMS is allowed to take the most stable conformation of the model compound.

On the other hand, PTMO has three crystal modifications, which were designated as I, II, and III.[37] In modifications I, II, and III, the PTMO chain adopts tttt, tgtt, and tggt conformations, respectively. The tgtt sequence of modification II repeats in such a manner as $(tg^+tt)(tg^-tt)$.... Modification I is hydrous. Modification III is known to be thermodynamically more stable than II. These tendencies agree with the conformational features of the unperturbed PTMO chain.

3.6. Conformations and Thermal Properties of Representative Polysulfides and Polyethers. In Table 10, the summary of conformational analyses of the polysulfides and polyethers that we have so far treated is tabulated. The item "conformation" shows the most stable conformations of the model compounds and the unperturbed and crystallized polymers. Except for PPS, the unperturbed polymers keep the conformational preferences of their model compounds. Most of the polymers crystallize to form the same conformations. The exceptions are PPS and PPO, which are forced to adopt the extended all-trans structure because of steric constraint by the methyl side chain. There is a possibility that crystal conformations of polymers without bulky side chains can be presumed from their Θ-state conformations or the most stable conformers of model compounds and vice versa.

The configurational entropy, S_{conf}, is given by[62−65]

$$S_{conf} = R\left[\ln z + T\frac{d(\ln z)}{dT}\right] \quad (17)$$

where z is the partition function per monomer mole:

$$z = Z^{1/x} = (J^* \prod_{i=2}^{n-1} U_i J)^{1/x} \quad (18)$$

Here, Z is the partition function of the whole chain, $J^* = [1\ 0\ 0]$, J is the column matrix whose elements are unity, and n is the number of skeletal bonds. The configurational energy is calculated from[66]

$$U_{conf} = RT^2\frac{d(\ln z)}{dT} \quad (19)$$

The S_{conf} and U_{conf} values at melting point correspond to differences in entropy and internal energy of the molecular chain between crystalline and molten states, respectively (viz., the intramolecular contributions to entropy and enthalpy of fusion, respectively). Shown in Table 10 are the S_{conf} and U_{conf} values calculated from eqs 17 and 19, together with experimental entropies (ΔS_u's) and enthalpies (ΔH_u's) of fusion. The equilibrium melting point, T_m, satisfies the relation of $T_m = \Delta H_u/\Delta S_u$.

The thermodynamic data of Table 10 may be summarized as follows. In the polysulfides and polyethers, the S_{conf} term accounts for 80−90% of ΔS_u. The entropy of fusion is mostly due to the configurational change between crystalline and molten states. As for PTMS, however, the S_{conf} value calculated here somewhat exceeds the observation of ΔS_u. Besides the experimental error, the following cause may be mentioned. In the S_{conf} calculation, the molten polymer is assumed to be completely random coil. In the PTMS melt, however, intramolecular and intermolecular attractions such as dipole−dipole interactions are formed to induce some local ordering, which would render the actual S_{conf} smaller than expected. For poly(methylene oxide) (PMO), PES, PEO, PTMS, and PTMO, which adopt the most stable conformations in the crystal, the intramolecular contributions (U_{conf}'s) to ΔH_u amount to ca. 30%. Accordingly, the residual 70% of ΔH_u stems from intermolecular interactions. However, the $U_{conf}/\Delta H_u$ ratio of PPO is no more than 15%, because PPO crystallizes to form the metastable all-trans structure.

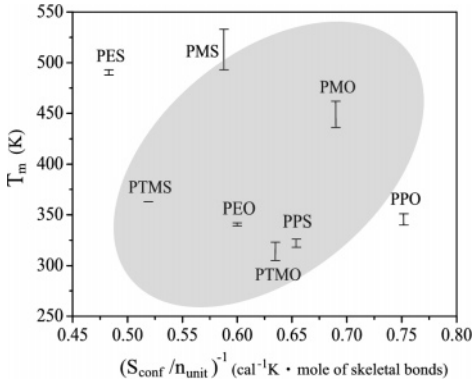

Figure 6. Correlation between melting point, T_m, and the reciprocal of configurational entropy per skeletal bond, $(S_{conf}/n_{unit})^{-1}$, of the polysulfides and polyethers. The error bar represents the range of reported T_m values.

3.7. Dipole-Dipole Interactions of the PES Crystal. In Figure 6, the melting points of the polymers are plotted against the reciprocal of configurational entropy per mole of skeletal bonds, $(S_{conf}/n_{unit})^{-1}$, where n_{unit} is the number of skeletal bonds in the repeating unit. If we note that $T_m = \Delta H_u/\Delta S_u \approx \Delta H_u/S_{conf}$, we can expect a positive correlation to be formed between T_m and $(S_{conf}/n_{unit})^{-1}$. Although the plot of Figure 6 is far from linear, at least, two data on PPO and PES are seen to be out of the correlation. As stated above, the crystallized PPO chain adopts the metastable ttt conformation. This leads to the comparatively large $(S_{conf}/n_{unit})^{-1}$ and small (U_{conf}/n_{unit}) values. On the other hand, the deviation for PES is due to the other factor, viz., enthalpy of fusion; the $\Delta H_u/n_{unit}$ value of PES is much larger than those of the others.

The PES chain crystallizes to adopt the particular g^+tg^- conformation,[46] in which a strong dipole moment is formed along the bisector of the C−S−C angle (see Figure 7). Because the dipole−dipole interactions are expected to stabilize the crystal structure, we calculated the interaction energy according to the following procedures.

(1) Seven dimeric models were located as in the PES crystal (orthorhombic, $a = 8.50$, $b = 4.95$, and c (fiber axis) $= 6.70$ Å, Figure 7a),[46] and the geometrical parameters were optimized by density functional calculations at the B3LYP/6-31G(d) level. Then, the covalent bonds were kept by the redundant treatment.[69] The optimum structure (Figure 7b) is somewhat distorted, but

Table 10. Conformations and Thermodynamic Quantities of Representative Polysulfides (X = S) and Polyethers (X = O)[a]

	$[-CH_2-X]_x$		$[-CH_2-CH_2-X]_x$		$[-CH_2-CH_2-CH_2-X]_x$		$[-CH_2-CH(CH_3)-X]_x$	
	PMS	PMO	PES	PEO	PTMS	PTMO	PPS	PPO
conformation[b]								
model compound[c]	gg[d]	gg[d]	$g^{\pm}tg^{\mp}$[e]	ttt, tgt[e]	gggg[f]	tggt[f]	g^-tg^-[g]	tg^+g^-[h]
Θ state[i]		gg[d]		tgt[e]	gggg[f]	tggt[f]	g^-tt[g]	tg^+g^-[h]
crystal	gg[j]	gg[k]	g^+tg^- [l]	tgt, ttt[m]	gggg[n]	tggt, tgtt, tttt[o]	ttt[p]	ttt[q]
S_{conf},[r] cal K^{-1} mol^{-1}	3.4	2.9	6.2	5.0	7.7	6.3	4.6	4.0
ΔS_u,[s] cal K^{-1} mol^{-1}		2.5−3.5	5.9−7.8	5.8−6.7	6.8	6.5−7.4		5.3−5.7
U_{conf},[t] kcal mol^{-1}	0.38	0.37	0.79	0.64	0.73	0.69	0.12	0.27
ΔH_u,[s] kcal mol^{-1}		1.1−1.6	2.9−3.8	2.0−2.3	2.5	2.1−2.3		1.8−2.0
T_m,[s] °C	220−260	163−189	215−220	66−69	90	32−50	45−53	67−78

[a] Abbreviations: PMS, poly(methylene sulfide); PMO, poly(methylene oxide); PES, poly(ethylene sulfide); PEO, poly(ethylene oxide); PTMS, poly(trimethylene sulfide); PTMO, poly(trimethylene oxide); PPS, poly(propylene sulfide); PPO, poly(propylene oxide). The blanks represent unavailable data. [b] The conformation represents a sequence of rotational isomeric states in the bonds of the above chemical formula. [c] The most stable conformers of model compounds, determined from MO calculations and NMR experiments. [d] Reference 14. [e] Reference 1. 1,2-Dimethoxyethane, a monomeric model of PEO, shows a weak trans preference (≤ 0.5 kcal mol^{-1}) in the C−C bond.[1,38,39] On the other hand, precise MO calculations at the MP2/6-311++G(3df, 3pd) level indicated that the C−C bond of the central repeating unit of a trimeric model compound of PEO, 1,2-bis(2-methoxyethoxy)ethane, has a conformational energy of −0.1 kcal mol^{-1}.[40] [f] This study. In the C−S bond of PTMS in the Θ state, the t, g^+ and g^- states are approximately equiprobable. [g] For (*R*)-1,2-bis(methylthio)propane and isotactic (*R*)-PPS.[23] [h] For (*R*)-1,2-dimethoxypropane and isotactic (*R*)-PPO.[24,41−43] [i] The most stable conformations in the individual bonds of the unperturbed polymers. The Θ states of PMS and PES have not been found. [j] Reference 44. [k] Reference 45. [l] Reference 46. The conformational sequence repeats reversely: $(g^+tg^-)(g^-tg^+)(g^+tg^-)$... [m] References 47−50. The ttt conformation is formed only in stretched samples. [n] References 6 and 7. [o] Reference 37. [p] For isotactic PPS. Reference 51. [q] For isotactic PPO. Reference 52. [r] According to eq 17. [s] See ref 53. [t] According to eq 19.

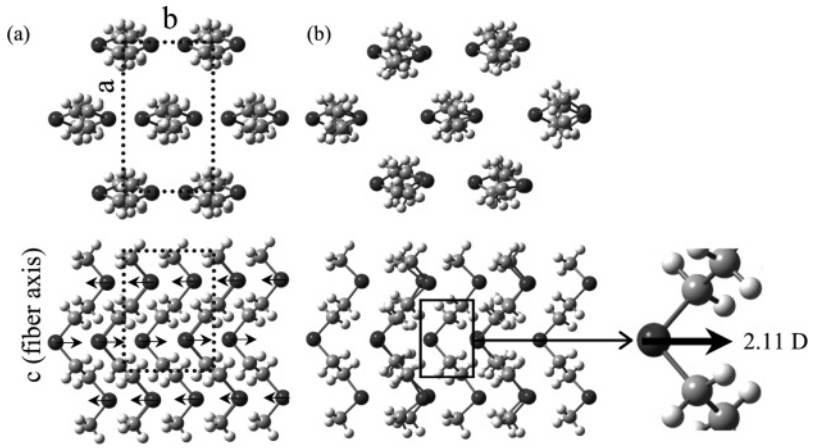

Figure 7. Dimer models for dipole moment evaluation: (a) initial (corresponding to the PES crystal) and (b) optimized structures. The arrows stand for the dipole moments. The dotted rectangles represent the unit cell.

the g^+tg^- conformation and the pseudohexagonal arrangement are preserved.

(2) The partial charge on each atom was calculated by the Merz−Singh−Kollman method[70,71] at the B3LYP/6-311+G-(2d,p) level. The dipole moment in the direction of the bisector of the C−S−C angle was evaluated from the partial charges of the central CH_2 −S−CH_2 part of the dimer located at the center of the pseudohexagon (Figure 7b), because this part is expected to be least perturbed by the edge and terminal effects and the closest to the corresponding part of the real crystal. The dipole moment per monomeric unit was obtained as 2.11 D (the partial charges: CH_2, +0.196; S, −0.392).

(3) The dipole−dipole interactions between $\vec{\mu}_1$ and $\vec{\mu}_j$'s were calculated from[72]

$$W = -\frac{1}{2}\sum_{n_x=1}^{N_{cell}}\sum_{n_y=1}^{N_{cell}}\sum_{n_x=1}^{N_{cell}}\frac{1}{4\pi\epsilon_0}\frac{3(\vec{r}_j\cdot\vec{\mu}_1)(\vec{r}_j\cdot\vec{\mu}_j) - (\vec{\mu}_1\cdot\vec{\mu}_j)\,r_j^2}{r_j^5} \quad (20)$$

where $\vec{\mu}_1$ is the dipole moment of interest, $\vec{\mu}_j$'s represent all dipole moments except $\vec{\mu}_1$ included in the N_{cell}^3 unit cells, and r_j is the distance between $\vec{\mu}_1$ and $\vec{\mu}_j$. There are N_{cell} cells in the *x*, *y*, and *z* directions, and $\vec{\mu}_1$ was placed in the central unit cell. The *x*, *y*, and *z* coordinates of the dipole moments were determined from the crystal structure (Figure 8).

The total and intramolecular dipole−dipole interaction energies were calculated as a function of N_{cell}. Because the interaction decreases in proportional to r_j^{-3}, both energies were obtained to be almost constant for $N_{cell} \geq 7$; the former and latter energies converge to −1.02 and −0.15 kcal mol^{-1}, respectively. Of the amount (on average, 3.4 kcal mol^{-1}) of ΔH_u of PES, ca. 0.8 kcal mol^{-1} comes from the configurational energy (U_{conf}), and hence $^1/_3$−$^1/_2$ of the rest; i.e., the intermolecular term is due to the dipole−dipole interactions, which raise the melting point of PES by ca. 150 °C ($|W|/\Delta S_u = 1.02 \times 10^3/6.9$).

Poly(ethylene sulfide) is soluble in only a few polar solvents such as nitrobenzene, *o*-dichlorobenzene, α-methylnaphthalene, dithiolane, and dimethyl sulfoxide above 140 °C.[73] The network of the dipole−dipole interactions is so strong that any solvent cannot dissolve the PES crystal at low temperatures. Above 140 °C, however, activated thermal motions allow the polar solvents to infiltrate the crystal and acquire the dipole interactions from the polymer segments. Accordingly, the thermostability and low solubility have the same origin.

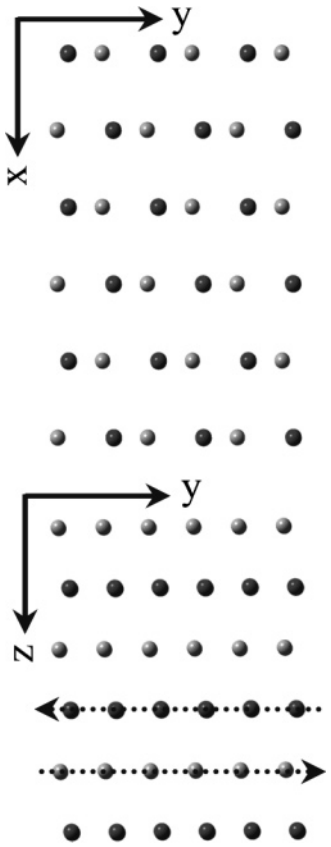

Figure 8. Positions of the dipole moments in the PES crystal of $N_{cell} = 3$. The *x*, *y*, and *z* directions are parallel to the *a*, *b*, and *c* axes of the unit cell. The dipole moments at the dark and light points have directions opposite to each other. μ_1 is placed in the central unit cell.

4. Concluding Remarks

In the polysulfides, the C−S bond and its adjoining C−C bond prefer the gauche state. As seen for PES, however, the strong S···S repulsion often gives rise to the apparent trans preference in the C−C bond. A variety of interactions due to the dipole moments are also characteristic of the polysulfides and the sources of their unique properties.

The C−C bond adjacent to the C−O bond of the polyethers has the inherent gauche preference due to the attractive gauche effect. As found for PEO and PPO, the polyethers often form the (C−H)···O attractions, whose strengths depend on the number of carbon atoms between ether linkages.[74,75] In some polyethers, the former factor appears predominantly, and the

latter is often superior in other polyethers. These tendencies, being sensitive to the environment, are changeable. This is why conformational characteristics of the polyethers have been difficult to understand and a subject of discussion and controversy.

Acknowledgment. This work was partly supported by the Asahi Glass Foundation.

References and Notes

(1) Sasanuma, Y.; Ohta, H.; Touma, I.; Matoba, H.; Hayashi, Y.; Kaito, A. *Macromolecules* **2002**, *35*, 3748.
(2) Foster, J. P.; Weinhold, F. *J. Am. Chem. Soc.* **1980**, *102*, 7211.
(3) Reed, A. E.; Curtiss, L. A.; Weinhold, F. *Chem. Rev.* **1988**, *88*, 899.
(4) Glendening, E. D.; Reed, A. E.; Carpenter, J. E.; Weinhold, F. *NBO* version 3.1. Theoretical Chemistry Institute and Department of Chemistry, University of Wisconsin: Madison, WI.
(5) Welsh, W. J.; Mark, J. E.; Riande, E. *Polym. J.* **1980**, *12*, 467.
(6) Sakakihara, H.; Takahashi, Y.; Tadokoro, H., *Discuss. Meeting Soc. Polym. Sci., Jpn., Tokyo, Prepr.* **1969**, 407.
(7) Tadokoro, H. *Structure of Crystalline Polymers;* Wiley & Sons: New York, 1979; Chapter 7.
(8) Frisch, M. J.; Trucks, G. W.; Schlegel, H. B.; Scuseria, G. E.; Robb, M. A.; Cheeseman, J. R.; Montgomery, Jr., J. A.; Vreven, T.; Kudin, K. N.; Burant, J. C.; Millam, J. M.; Iyengar, S. S.; Tomasi, J.; Barone, V.; Mennucci, B.; Cossi, M.; Scalmani, G.; Rega, N.; Petersson, G. A.; Nakatsuji, H.; Hada, M.; Ehara, M.; Toyota, K.; Fukuda, R.; Hasegawa, J.; Ishida, M.; Nakajima, T.; Honda, Y.; Kitao, O.; Nakai, H.; Klene, M.; Li, X.; Knox, J. E.; Hratchian, H. P.; Cross, J. B.; Bakken, V.; Adamo, C.; Jaramillo, J.; Gomperts, R.; Stratmann, R. E.; Yazyev, O.; Austin, A. J.; Cammi, R.; Pomelli, C.; Ochterski, J. W.; Ayala, P. Y.; Morokuma, K.; Voth, G. A.; Salvador, P.; Dannenberg, J. J.; Zakrzewski, V. G.; Dapprich, S.; Daniels, A. D.; Strain, M. C.; Farkas, O.; Malick, D. K.; Rabuck, A. D.; Raghavachari, K.; Foresman, J. B.; Ortiz, J. V.; Cui, Q.; Baboul, A. G.; Clifford, S.; Cioslowski, J.; Stefanov, B. B.; Liu, G.; Liashenko, A.; Piskorz, P.; Komaromi, I.; Martin, R. L.; Fox, D. J.; Keith, T.; Al-Laham, M. A.; Peng, C. Y.; Nanayakkara, A.; Challacombe, M.; Gill, P. M. W.; Johnson, B.; Chen, W.; Wong, M. W.; Gonzalez, C.; Pople, J. A *Gaussian03*, revision C.02. Gaussian, Inc.: Wallingford CT, 2004.
(9) Foresman, J. B.; Frisch, A. E. *Exploring Chemistry with Electronic Structure Methods*, 2nd ed.; Gaussian, Inc.: Pittsburgh, PA, 1996.
(10) Roberts, R. M.; Cheng, C. C. *J. Org. Chem.* **1958**, *23*, 983.
(11) Budzelaar, P. H. M. *gNMR*, version 5.0. IvorySoft & Adept Scientific plc: Letchworth, U.K., 2004.
(12) Sasanuma, Y.; Hattori, S.; Imazu, S.; Ikeda, S.; Kaizuka, T.; Iijima, T.; Sawanobori, M.; Azam, M. A.; Law, R. V.; Steinke, J. H. G. *Macromolecules* **2004**, *37*, 9169.
(13) Sasanuma, Y.; Teramae, F.; Yamashita, H.; Hamano, I.; Hattori, S. *Macromolecules* **2005**, *38*, 3519.
(14) Sawanobori, M.; Sasanuma, Y.; Kaito, A. *Macromolecules* **2001**, *34*, 8321.
(15) Inomata, K.; Phataralaoha, N.; Abe, A. *Comput. Polym. Sci.* **1991**, *1*, 126.
(16) Flory, P. J. *Statistical Mechanics of Chain Molecules;* Interscience: New York, 1969.
(17) Mattice, W. L.; Suter, U. W. *Conformational Theory of Large Molecules: The Rotational Isomeric State Model in Macromolecular Systems*; Wiley & Sons: New York, 1994.
(18) Born, M. *Z. Phys.* **1920**, *1*, 45.
(19) Israelachvili, J. N. *Intermolecular and Surface Forces With Applications to Colloidal and Biological Systems*; Academic: New York, 1985; Chapter 4.
(20) Onsager, L. *J. Am. Chem. Soc.* **1936**, *58*, 1486.
(21) Wong, M. W.; Frisch, M. J.; Wiberg, K. B. *J. Am. Chem. Soc.* **1991**, *113*, 4776.
(22) See, for sample, section 3.6 of ref 1. In the optimization here, no weights were used.
(23) Sasanuma, Y.; Hayashi, Y.; Matoba, H.; Touma, I.; Ohta, H.; Sawanobori, M.; Kaito, A. *Macromolecules* **2002**, *35*, 8216.
(24) Law, R. V.; Sasanuma, Y. *Macromolecules* **1998**, *31*, 2335.
(25) Konishi, T.; Yoshizaki, T.; Yamakawa, H. *Macromolecules* **1991**, *24*, 5614.
(26) Yamakawa, H. *Modern Theory of Polymer Solutions;* Harper & Row: New York, 1971; Chapter 6.
(27) Sánchez, A.; Bello, A.; Marco, C.; Fatou, J. G. *Makromol. Chem.* **1988**, *189*, 399.
(28) Chiu, D. S.; Takahashi, Y.; Mark, J. E. *Polymer* **1976**, *17*, 670.
(29) Takahashi, Y.; Mark, J. E. *J. Am. Chem. Soc.* **1976**, *98*, 3756.
(30) Guzman, J.; Riande, E.; Welsh, W. J.; Mark, J. E. *Makromol. Chem.* **1982**, *183*, 2573.
(31) Riande, E.; Saiz, E. *Dipole Moments and Birefringence of Polymers;* Prentice Hall: Englewood Cliffs, NJ, 1992; Chapter 4.
(32) Mark, J. E.; Chiu, D. S. *J. Chem. Phys.* **1977**, *66*, 1901.
(33) Abe, A.; Mark, J. E. *J. Am. Chem. Soc.* **1976**, *98*, 6468.
(34) Abe, A.; Ichimura, N.; Shinohara, T.; Furuya, H. *J. Mol. Struct.* **1995**, *350*, 129.
(35) Juaristi, E. *Introduction to Stereochemistry and Conformational Analysis*; Wiley & Sons: New York, 1991; Chapter 18.
(36) Juaristi, E.; Cuevas, G. *The Anomeric Effect;* CRC Press: Boca Raton, FL, 1995; Chapter 4.
(37) Tadokoro, H.; Takahashi, Y.; Chatani, Y.; Kakida, H. *Makromol. Chem.* **1967**, *109*, 96.
(38) Tsuzuki, S.; Uchimaru, T.; Tanabe, K.; Hirano, T. *J. Phys. Chem.* **1993**, *97*, 1346.
(39) Jaffe, R. L.; Smith, G. D.; Yoon, D. Y. *J. Phys. Chem.* **1993**, *97*, 12745.
(40) Sasanuma, Y. Intramolecular Interactions of Polyethers and Polysulfides, Investigated by NMR, Ab Initio Molecular Orbital Calculations, and Rotational Isomeric State Scheme: An Advanced Analysis of NMR Data. In *Annual Reports on NMR Spectroscopy*; Webb, G. A., Ed.; Academic Press: New York, 2003; Vol. 49; Chapter 5.
(41) Sasanuma, Y. *J. Phys. Chem.* **1994**, *98*, 13486.
(42) Sasanuma, Y. *Macromolecules* **1995**, *28*, 8629.
(43) Sasanuma, Y.; Iwata, T.; Kato, Y.; Kato, H.; Yarita, T.; Kinugasa, S.; Law, R. V. *J. Phys. Chem. A* **2001**, *105*, 3277.
(44) Carazzolo, G.; Valle, G. *Makromol. Chem.* **1966**, *90*, 66.
(45) Uchida, T.; Tadokoro, H. *J. Polym. Sci., Part A-2* **1967**, *5*, 63.
(46) Takahashi, Y.; Tadokoro, H.; Chatani, Y. *J. Macromol. Sci., Phys.* **1968**, *B2*, 361.
(47) Tadokoro, H.; Chatani, Y.; Yoshihara, T.; Tahara, S.; Murahashi, S. *Makromol. Chem.* **1964**, *73*, 109.
(48) Takahashi, Y.; Tadokoro, H. *Macromolecules* **1973**, *6*, 672.
(49) Takahashi, Y.; Sumita, I.; Tadokoro, H. *J. Polym. Sci., Polym. Phys. Ed.* **1973**, *11*, 2113.
(50) Tashiro, K.; Tadokoro, H. *Rep. Prog. Polym. Phys. Jpn.* **1978**, *21*, 417.
(51) Sakakihara, H.; Takahashi, Y.; Tadokoro, H.; Sigwalt, P.; Spassky, N. *Macromolecules* **1969**, *2*, 515.
(52) Cesari, M.; Perego, G.; Marconi, W. *Makromol. Chem.* **1966**, *94*, 194.
(53) We searched the PolyInfo Database for the thermodynamic data. The database service is provided by the Materials Information Technology Station of the National Institute for Materials Science, Japan (http://polymer.nims.go.jp/). The literature on PMS,[54] PMO,[55] PES,[56] PEO,[57] PTMS,[58] PTMO,[59] PPS,[60] and PPO[61] are listed below.
(54) (a) Lal, J.; Trick, G. S. *J. Polym. Sci.* **1961**, *50*, 13. (b) Gipstein, E.; Wellisch, E.; Sweeting, O. J. *J. Polym. Sci., Part B* **1963**, *1*, 237. (c) Lando, J. B.; Stannett, V. *J. Polym. Sci., Part B* **1964**, *2*, 375. (d) Frosini, V.; Butta, E.; Calamia, M. *J. Appl. Polym. Sci.* **1967**, *11*, 527.
(55) (a) Inoue, M. *J. Polym. Sci.* **1961**, *51*, 18. (b) Iguchi, M. *Makromol. Chem.* **1976**, *177*, 549. (c) Hay, J. N. *J. Polym. Sci., Polym. Chem. Ed.* **1976**, *14*, 2845. (d) Wunderlich, B.; Gaur, U. *Pure Appl. Chem.* **1980**, *52*, 445. (e) Zihlif, A. M. *Mater. Chem. Phys.* **1985**, *13*, 21. (f) Runt, J.; Wagner, R. F.; Zimmer, M. *Macromolecules* **1987**, *20*, 2531. (g) Koszkul, J. *J. Therm. Anal.* **1992**, *38*, 2311. (h) Plummer, C. J. G.; Menu, P.; Cudre-Mauroux, N.; Kausch, H. H. *J. Appl. Polym. Sci.* **1995**, *55*, 489.
(56) (a) Nicco, A.; Machon, J. P.; Fremaux, H.; Pied, J. P.; Zindy, B.; Thiery, M. *Eur. Polym. J.* **1970**, *6*, 1427. (b) Bhaumik, D.; Mark, J. E. *Macromolecules* **1981**, *14*, 162.
(57) (a) Mandelkern, L. *Chem. Rev.* **1956**, *56*, 903. (b) Braun, W.; Hellwege, K. H.; Knappe, W. *Kolloid, Z. Z. Polym.* **1967**, *215*, 10. (c) Part b of ref 56. (d) Maurya, K. K.; Srivastava, N.; Hashmi, S. A.; Chandra, S. *J. Mater. Sci.* **1992**, *27*, 6357. (e) Lommerts, B. J.; Klop, E. A.; Aerts, J. *J. Polym. Sci., Part B: Polym. Phys.* **1993**, *31*, 1319. (f) Qiu, W.; Pyda, M.; Nowak-Pyda, E.; Habenschuss, A.; Wunderlich, B. *Macromolecules* **2005**, *38*, 8454.
(58) Sánchez, A.; Marco, C.; Fatou, J. G.; Bello, A. *Eur. Polym. J.* **1988**, *24*, 355.
(59) (a) Yoshida, S.; Sakiyama, M.; Seki, S. *Rep. Prog. Polym. Phys. Jpn.* **1969**, *12*, 247. (b) Perez, E.; Fatou, J. G..; Bello, A. *Eur. Polym. J.* **1987**, *23*, 469.
(60) (a) Reference 51. (b) Lai, J.; Trick, G. S. *J. Polym. Sci., Part A-1* **1970**, *8*, 2339.
(61) (a) Beaumont, R. H.; Clegg, B.; Gee, G.; Herbert, J. B. M.; Marks, D. J.; Roberts, R. C.; Sims, D. *Polymer* **1966**, *7*, 401. (b) Booth, C.; Devoy, C. J.; Gee, G. *Polymer* **1971**, *12*, 327.
(62) Brant, D. A.; Miller, W. G.; Flory, P. J. *J. Mol. Biol.* **1967**, *23*, 47.
(63) Tonelli, A. E. *J. Chem. Phys.* **1970**, *52*, 4749; *53*, 4339.
(64) Mark, J. E. *J. Chem. Phys.* **1977**, *67*, 3300.
(65) Abe, A. *Macromolecules* **1980**, *13*, 546.

CDV

(66) The partition function of the whole chain can be defined as

$$Z = \sum_{k}^{K} \exp(-E_k/RT)$$

where k represents the configuration (a sequence of conformations) of the polymeric chain, and E_k is the corresponding internal energy.[67] From the above equation and eq 17, the configurational entropy of the whole chain is given as

$$S_{\mathrm{conf}} = R \ln Z + \frac{1}{T}\sum_{k}^{K} E_k \frac{\exp(-E_k/RT)}{Z}$$

$$= R \ln Z + \frac{U(T) - U_{\mathrm{cryst}}}{T}$$

where $U(T)$ is the internal energy of the random coil in the Θ state at T (K) and U_{cryst} is that of the crystallized chain. This equation is equivalent to the well-known expression of entropy.[68] Here, the E_k value must be defined with respect to that of the crystal conformation so as to satisfy $E_{\mathrm{cryst}} = 0$. Comparison between the above equation and eq 17 yields $U(T) - U_{\mathrm{cryst}} \equiv U_{\mathrm{conf}} = RT^2[\mathrm{d}(\ln Z)/\mathrm{d}T]$. It is assumed that all possible conformations of the molten polymer reach equilibrium at the melting point. Adoption of z in eq 18, instead of Z, gives the S_{conf} and U_{conf} values in the unit of per monomer mole because $\ln z = \ln Z^{1/x} = (1/x) \ln Z$.

(67) In our studies, conformational energies have been derived from the ΔG_k values to discuss the conformational equilibrium. However, eqs 17 and 19 require the internal energies to yield the S_{conf} and U_{conf} values. Conformer internal energies of BMTP were calculated from ab initio MO calculations at MP2/6-311+G(3df,2p)//HF/6-31G(d) level, and broken down into the three conformational energies: $E_\rho = -0.25$, $E_\sigma = -0.30$, and $E_\omega = 0.99$ kcal mol^{-1}. These energy parameters gave an S_{conf} value of 7.6_3 cal mol^{-1} K^{-1}, and the conformational energies in the column of "ΔG_k" of Table 5 yielded $S_{\mathrm{conf}} = 7.6_0$ cal mol^{-1} K^{-1}. Therefore, the conformational energies determined so far for the experimental observations were used as they are to calculate the S_{conf} and U_{conf} values.

(68) Atkins, P. W. *Physical Chemistry*, 6th ed.; Oxford University Press: New York, 1998; Chapter 20.
(69) Peng, C.; Ayala, P. Y.; Schlegel, H. B.; Frisch, M. J. *J. Comput. Chem.* **1996**, *17*, 49.
(70) Besler, B. H.; Merz, K. M., Jr.; Kollman, P. A. *J. Comput. Chem.* **1990**, *11*, 431.
(71) Singh, U. C.; Kollman, P. A. *J. Comput. Chem.* **1984**, *5*, 129.
(72) Kittel, C. *Introduction to Solid State Physics*, 5th ed.; Wiley & Sons: New York, 1976; Chapter 13.
(73) Masamoto, J. Poly(ethylene sulfide). In *Polymer Data Handbook;* Mark, J. E., Ed.; Oxford University Press: New York, 1999; p 553.
(74) Law, R. V.; Sasanuma, Y. *J. Chem. Soc., Faraday Trans.* **1996**, *92*, 4885.
(75) Sasanuma, Y.; Ono, T.; Kuroda, Y.; Miyazaki, E.; Hikino, K.; Arou, J.; Nakata, K.; Inaba, H.; Tozaki, K.; Hayashi, H.; Yamaguchi, K. *J. Phys. Chem. B* **2004**, *108*, 13163.

MA0523623